ELSEVIER

Materials Science and Engineering A 447 (2007) 150–157

MATERIALS SCIENCE & ENGINEERING A

www.elsevier.com/locate/msea

Uniform and graded chemical milling of aluminum foams

Y. Matsumoto [a,*], A.H. Brothers [b], S.R. Stock [c], D.C. Dunand [b]

[a] *Department of Mechanical Engineering, Oita National College of Technology, 1666 Maki, Oita 870-0152, Japan*
[b] *Department of Materials Science and Engineering, Northwestern University, 2220 Campus Drive, Evanston, IL 60208-3108, USA*
[c] *Department of Molecular Pharmacology and Biological Chemistry, Northwestern University, 303 East Chicago Avenue, Chicago, IL 60611-3008, USA*

Received 29 May 2006; received in revised form 2 September 2006; accepted 19 October 2006

Abstract

Commercial open-cell aluminum alloy foams are subjected to chemical dissolution to reduce their density. Dissolution rates are measured for various pH, temperature and alloy heat-treatment conditions, and the resulting foam structures and surface conditions are evaluated by microscopy and X-ray microcomputed tomography to identify conditions which minimize corrosive damage. The effect of uniform dissolution on foam compressive mechanical properties is interpreted in terms of these observations. A method for production of density-graded foam samples from uniform-density precursors is also demonstrated.

Keywords: Metallic foams; Al-6101; Functionally graded materials; Chemical machining; Chemical milling; Corrosion; Mechanical properties

1. Introduction

Metallic foams are used in sandwich panels and other lightweight structural components, in energy absorption systems for impact protection, as heat sinks for electronic devices, and as acoustic insulation [1,2]. Advances in metallic foam processing have historically focused on improving uniformity in foam structure and properties, and variations in local density or architecture have been avoided as undesirable [1,2]. Recent work, however, indicates that in certain cases (e.g., structural components [3–5], biomaterials [6], electrode materials [7,8] and heat transfer devices [6]) controlled-density gradients allow for improved foam performance as compared to uniform-density foams of equal mass.

In response to this development, several approaches to density-grading of low-density metallic foams have been studied, and processing methods are now available for density-graded Cu [6,9], Ni [7], Mg [10] and Al [4,11] foams. In this report, we consider a new method based on chemical dissolution (chemical milling) of uniform-density metallic foams, which produces continuous density gradients and which may be simpler to implement than previous methods, in which density-grading is performed concurrently with foaming. The influence of processing conditions (e.g., solution pH, temperature and alloy temper) on chemical dissolution of commercial open-cell aluminum alloy foams was documented. The effect of dissolution on foam structure and surface condition was also examined, and the least-damaging dissolution conditions were assessed using microscopy, X-ray microcomputed tomography and mechanical properties measurements. By continuously removing a dissolution bath from a container in which foams were suspended, a method for continuously grading foam relative density from 10 to 5% was demonstrated.

2. Experimental procedures

2.1. Uniform dissolution

Duocel® reticulated aluminum foam sheets were fabricated from 6101 aluminum alloy (hereafter, Al-6101) by ERG Aerospace (Oakland, CA, USA) using a casting method described by Ashby et al. [1]. The nominal pore density of the foam sheets was 0.8 pores/mm (20 pores per inch), and the nominal relative density was 10%. Bulk alloy specimens were cut from Al-6101-T61 extruded bus bar with a rectangular section of 6.35 mm × 50.8 mm, manufactured by Central Steel & Wire Company (Chicago, IL, USA). The chemical compositions of the foam and bulk alloy are shown in Table 1. For comparison, the nominal chemical composition of Al-6101

* Corresponding author. Tel.: +81 97 552 7481; fax: +81 97 552 6975.
E-mail address: matumoto@oita-ct.ac.jp (Y. Matsumoto).

0921-5093/$ – see front matter © 2006 Elsevier B.V. All rights reserved.
doi:10.1016/j.msea.2006.10.049

Table 1
Chemical composition (wt.%) of bulk and foamed Al-6101

Sample	Cu	Mg	Mn	Si	Fe	Zn	B	Others	Al
Nominal composition	0.10 (max.)	0.35–0.80	0.03 (max.)	0.30–0.70	0.50 (max.)	0.10 (max.)	0.06 (max.)	0.10 (max.)	Bal.
20PPI foam	0.03	0.22	0.01	0.20	0.10	0.01	0.03	–	99.38
Bulk alloy	0.04	0.47	0.02	0.29	0.18	0.01	0.04	–	98.93

[12] is also given. After fabrication, the foams were given a T6 heat-treatment by the manufacturer. This treatment involves solutionizing at 527 °C for 8 h, prior to water quenching and aging at 177 °C for 8 h to induce age hardening by Mg_2Si precipitates. To investigate the influence of these precipitates on corrosion and dissolution characteristics, an additional solution treatment (ST) at 530 °C for 30 min (for foams) or 1 h (for plates) was given to certain samples.

Quadrilateral foam samples (ca. 10 mm × 10 mm × 5 mm) were cut using a diamond saw from an as-received foam sheet and immersed in stirred 1000 mL baths of aqueous HCl or NaOH, whose pH was set and monitored using a pH meter equipped with a glass electrode. Changes in solution pH (towards neutrality) were observed during dissolution experiments, particularly at low HCl and NaOH concentrations. Therefore, solutions were replaced at intervals of less than 15 h for the pH 3 HCl solution (in which the average pH change was $+0.082\,h^{-1}$) and the pH 10 NaOH solution (average pH change $-0.21\,h^{-1}$). In the more concentrated solutions, with rates of pH change of $+0.003\,h^{-1}$ (pH 1) to $-0.015\,h^{-1}$ (pH 13), the solutions were replaced whenever necessary, in order to maintain their pH values within 15% of the target values.

Mass losses were measured after every few hours of immersion, after washing in deionized water and ethanol, and drying. Dissolution rates were then estimated from mass losses using manufacturer provided data for foam surface areas, under the assumption of uniform corrosion. These specific surface areas decreased with relative density, and the values were 19.0, 17.4, 15.3 and 12.3 cm^2/cm^3 for 10, 8, 6 and 4% dense foams, respectively. Interpolated specific surface areas were used for the estimate of true mass losses. In addition, such data were used when necessary, in order to convert mass loss to linear dissolution rate (i.e., thinning velocity). For comparison purposes, bulk coupons (6 mm × 25 mm × 1.5 mm) of known surface area were cut from extruded plates, polished with 1200 grit SiC paper, cleaned and subjected to the same series of dissolution conditions. These experiments were carried out for various temperatures and pH values by varying the concentration of HCl or NaOH in the baths.

2.2. Structural analysis

The effects of dissolution on foam architecture and surface condition were evaluated using optical and scanning electron microscopy (SEM, Hitachi S3500-N). In addition, certain foam specimens were selected for detailed analysis using a commercial microcomputed tomography (μCT) system (μCT 40, Scanco Medical, Bassersdorf, Switzerland) with a white X-ray source operating at an accelerating voltage and source current of 45 kV and 177 μA, respectively. For each of these specimens, five volumes (thin slabs with thickness ca. 600 μm and spanning the entire cross-section, equally spaced along the gauge length) were reconstructed with an isotropic spatial resolution near 15 μm. The data were binarized using the threshold value which gave greatest correspondence between the calculated tomographic relative density, averaged over all five volumes and the relative density measured by dry mass and dimensions for an as-received foam sample. The densities of the two other specimens, which had been solutionized and dissolved in NaOH solution of pH 13 (the reasons for this are discussed in further detail below), were then evaluated using the same threshold value. Two structural indices, the mean trabecular (i.e., strut) thickness and the structure model index were evaluated using the μCT software package. The details of these calculations are described elsewhere [13,14], but it is noted that both algorithms were designed for model-independent quantitative analysis of trabecular bone, whose structure is quite similar to that of Duocel® foams.

2.3. Mechanical properties

A series of foam specimens (all in the T6 condition for mechanical testing, though some samples had been solutionized before dissolution) was tested in displacement-controlled uniaxial compression at a nominal strain rate of $10^{-3}\,s^{-1}$. Each specimen had a rectangular cross-section and a minimum dimension seven times the pore size or greater, to avoid statistical variation in foam properties [1]. However, due to the limited dimensions of the as-received foam sheet, and the fact that the specimen longitudinal direction was kept perpendicular to the sheet plane to minimize the effects of anisotropy, the specimens were limited to aspect ratios averaging 1.3.

In most cases (11 of 15 tested specimens), the linear initial loading regions of the stress–strain curves were separated from the subsequent plateau regions by a local maximum in flow stress. In these cases, this local maximum stress was taken as the foam strength. In the remaining specimens (4 of 15), no distinct maximum stress was found, the transition between initial loading and plateau regions being essentially monotonic. In these cases, foam strength was determined by the intercept of two tangent lines extrapolated from the initial loading and plateau regions of the stress–strain curves. Initial stiffness in the foam specimens was determined using data from several loading/unloading cycles taken near the point of macroscopic yield, after compensation for load train compliance. Complete unloading was avoided during these cycles to prevent sample resettling, and data near the maximum applied stress were discarded to avoid the effects of plasticity.

2.4. Graded dissolution

A pH- and temperature-controlled NaOH bath was used to investigate density-grading of a foam by dissolution. Controlled, gravity-driven removal of the dissolution bath through an exhaust pipe produced a constant rate of decrease in the fluid level of a bottle in which a foam sample was maintained fixed, thus producing within the foam a longitudinal gradient in exposure time to the solution. Specifically, a T6-treated sample of size 19 mm × 5 mm × 50 mm was graded by this method. The measured rate of change of the relative density of this sample during uniform dissolution in pH 13 NaOH at room temperature was 1.1% h^{-1}. Therefore, a rate of change of fluid level of 6 mm/h was chosen to grade the foam sample to one-half its initial relative density over a length of about 27 mm. Although a slight decrease in the bath pH was observed during this grading process, it was not necessary to replace the solution, because the large bath volume (2000 mL) kept the pH value within 1% of its target value (pH 13) throughout the experiment. The resulting graded foam sample was mounted in an epoxy resin and polished to a 0.1 μm finish using an aqueous Al_2O_3 suspension. The longitudinal gradient in area fraction of the foam struts was measured by image analysis, from which the change in relative density was evaluated.

3. Results and discussion

3.1. Relative density and mass loss

Decreases in relative density with immersion time were evaluated for open-cell Al-6101 foams using HCl and NaOH solutions of varying concentration, as shown in Fig. 1. Initial foam relative densities were in the range of 10–13%, except for the two specimens dissolved at pH 3, which had higher initial relative densities of 14.1 and 15.7%; to illustrate differences in dissolution rate (i.e., slope) between specimens, the data are normalized by initial foam relative density. After about 1 week of immersion, measurable density changes occurred in foams exposed to solutions with pH outside the range ca. 3–10. As expected, dissolution rates increased quickly as pH values moved farther from neutrality. Dissolution rates were similar for both heat-treatments (T6 and ST, represented by square and circle symbols, respectively), though slightly accelerated dissolution was sometimes noted in T6-treated samples. Possibly, damage through preferential attack near the grain boundaries and precipitates in T6 samples caused this acceleration.

The fastest dissolution rates were observed in NaOH solutions of pH 11–13 (Fig. 1a). The rate of change in relative density at pH 13, for instance, was nearly 50 times greater than the rate of change at pH 1 (Fig. 1b). Accordingly, it was determined that dissolution in strong NaOH solutions offers the greatest potential for density reduction or grading of Al-6101 foams on practical timescales, and these dissolution conditions were selected for further analysis. As discussed in later sections, structural damage (e.g., strut fracture by preferential attack at grain boundaries or Mg_2Si precipitates) and the resulting deterioration of mechanical properties were also less severe after dissolution in alkaline solutions.

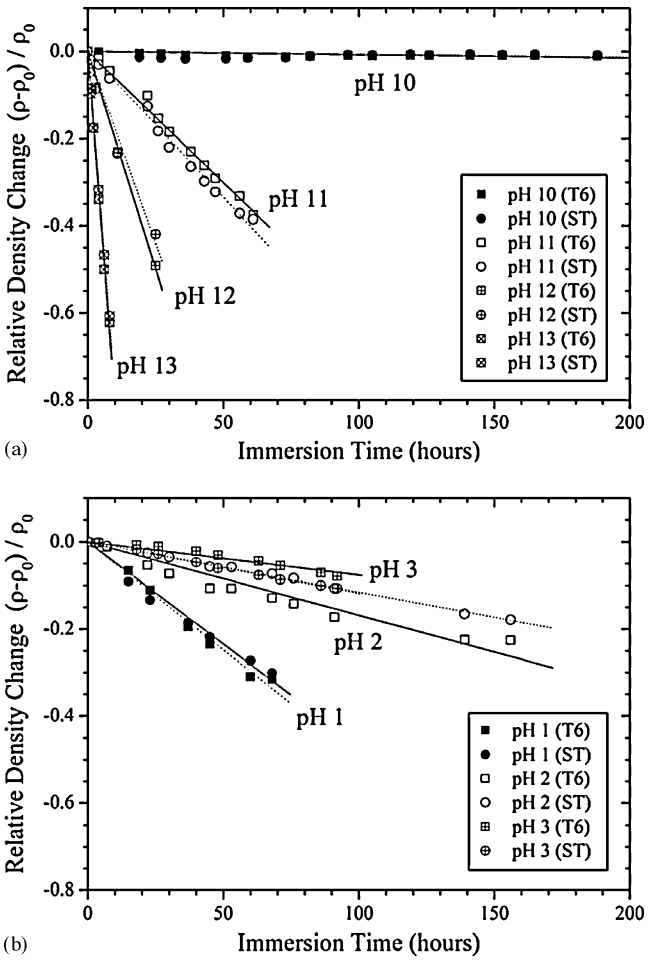

Fig. 1. Relative density changes for foams immersed in: (a) NaOH and (b) HCl solutions with various pH values at 23 °C. Data are normalized by the initial foam densities in order to illustrate the differences in slope more clearly.

Direct measurement of dissolution rates in foam specimens (Fig. 1) can be avoided if the relationship between dissolution rates in foamed and monolithic specimens is known, either by testing of bulk specimens or using literature data. To this end, dissolution rates in extruded Al-6101 sheet were measured under the same conditions shown in Fig. 1a, and the results are shown in Fig. 2. The dissolution rates in the bulk material were similar to those measured in foams consisting mainly of thin struts, indicating that there was no significant size effect in the dissolution rate. Recently, Sakashita et al. [15] reported a diameter dependency in the dissolution of high-carbon steel wire in aqueous NaCl solution, and explained that effect based on reduction of dissolved oxygen or promotion of a cathodic reaction involving hydrogen ions. It is likely that the dissolution mechanisms for Al-6101 in NaOH are quite different from those of steel in NaCl, explaining this discrepancy.

Fig. 3 shows dissolution rates calculated from mass loss results in NaOH solutions of various pH. For alkali pH between 10 and 12, the dissolution rate increased near linearly from ~0 to ~15 mm/year. However, in pH 13 solutions, the dissolution rate

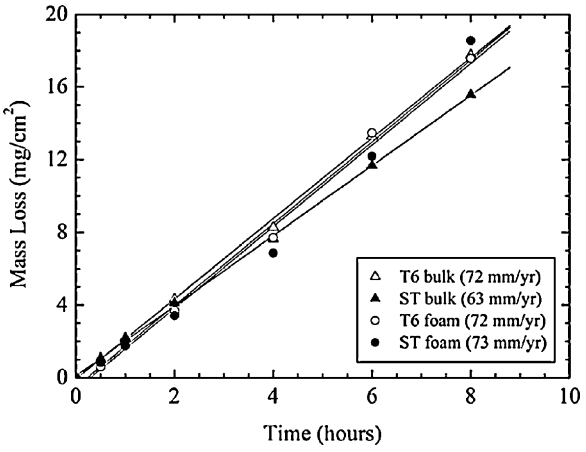

Fig. 2. Changes in mass (normalized by area) with immersion time in pH 13 NaOH solutions at 23 °C for Al-6101 foams and bulk specimens. Calculated dissolution rates are given in the figure legend.

accelerated to ∼70 mm/year (∼8 μm/h). It has been reported [12] that general-use 1100-H14 aluminum alloy shows an average dissolution rate of 2 mm/year or more in NaOH solutions exceeding pH 11, and this rate increases rapidly with a further rise of pH. Although dissolution of the present Al-6101 (a high-strength electric conduction material) in NaOH solution is not well documented, it is noted that T6 and ST foams seem to have a more rapid penetration rate of 4–5 mm/year at pH 11, as compared to Al-1100-H14.

3.2. Strut surfaces and foam structure

Although the mechanical properties of reticulated aluminum foams have been studied extensively (as summarized, e.g., in ref. [1]), there is little knowledge about the effect of strut surface condition on foam properties. Nonetheless, it is plausible that the quality of the surfaces in a dissolved or corroded foam will affect overall mechanical properties, because: (i) during strut bending, the dominant deformation mode in low-density foams

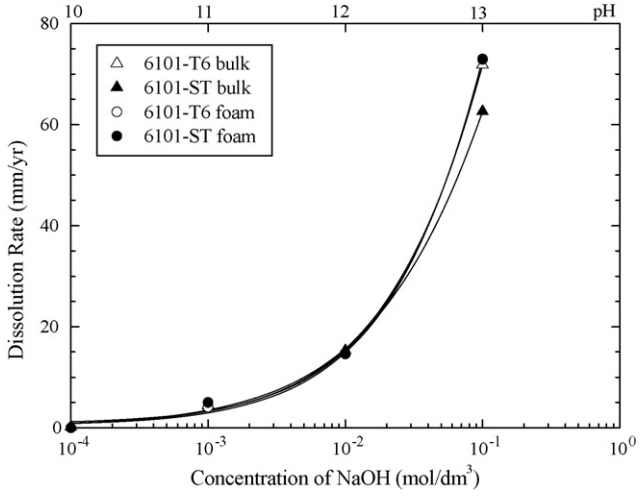

Fig. 3. Dissolution rates as a function of NaOH concentration (molarity and pH) for Al-6101 foams and bulk specimens at 23 °C.

[1], deformation initiates at strut surfaces where the local strain is highest; (ii) most deformation, at least at low strains, is concentrated in the struts, whose low thickness renders surface effects proportionally more important; (iii) corrosive damage may extend beyond the surfaces in certain cases, such as grain pull-out or severe pitting. Achieving maximum performance from partially dissolved aluminum foams therefore requires identifying the least-damaging immersion conditions, as discussed below.

Figs. 4a–d shows SEM images of T6- and solution-treated Al-6101 foams (initial relative density 9.7%) after dissolution in a room temperature HCl solution of pH 2. A layer of corrosion product (made particularly apparent by contrast with NaOH-treated foams; Figs. 5–6) is visible on all alloy surfaces, and evidence of large-scale damage in the form of sharp crack-like pits and grain pullout is seen in several places on the T6-treated specimen (Fig. 4a). Though the number and severity of these damaged regions were decreased by the solution treatment (Fig. 4c), the corrosion product remained and several deep pits and large area reductions were still visible, identifying HCl as a highly damaging immersion solution.

Figs. 5a–d shows SEM images of T6-treated Al-6101 foams (initial relative density 9.5%) after dissolution in a pH 13 NaOH solution at room temperature. Shallow, hemispherical corrosion pits were uniformly distributed on the surfaces of struts and nodes. Although one fifth of the foam mass had been dissolved (reducing the relative density of the foam, shown in Fig. 5b, from 9.5 to 7.5%), struts with sharp edges remained. These edges have largely disappeared from the struts of the foam having relative density 5% (Fig. 5d), while the hemispherical pits on grain boundaries become larger and etched grain boundaries are visible. Struts appeared to preferentially thin near the middle of their lengths, and at times were even interrupted by complete dissolution of their thinnest section.

Solution-treated Al-6101 foams (initial relative density 9.7%) were investigated in the same manner, as shown in Figs. 6a–d. The density of the hemispherical corrosion pits decreased, and strut and node surfaces with minimal damage and shallow pit depth were obtained. Even in foams reduced to relative densities of 5%, sharp strut edges remained and grain boundaries were not etched. Thus, after solution treatment was performed to solutionize Mg_2Si precipitates, Al-6101 foams were dissolved more uniformly, and reductions in strut and node sizes were possible without significant visible damage, despite the fact that this was the most rapid dissolution medium identified earlier (Fig. 1).

The foam samples shown in Fig. 6 were analyzed tomographically, along with a solution-treated as-received sample, and the results of this analysis (values are averages over the five thin-slab volumes taken from each sample and errors are standard deviations) are summarized in Table 2. Tomographic relative densities measured on each slab were within 8% relative deviation from those measured by mass and dimensions in each case (though the as-received sample was used for threshold calibration), with magnitude of standard deviations less than 0.1% for measurements within each slab. With decreasing relative density, mean strut thickness decreased, as expected. The values calculated for mean strut thickness are also in rough agreement with pre-

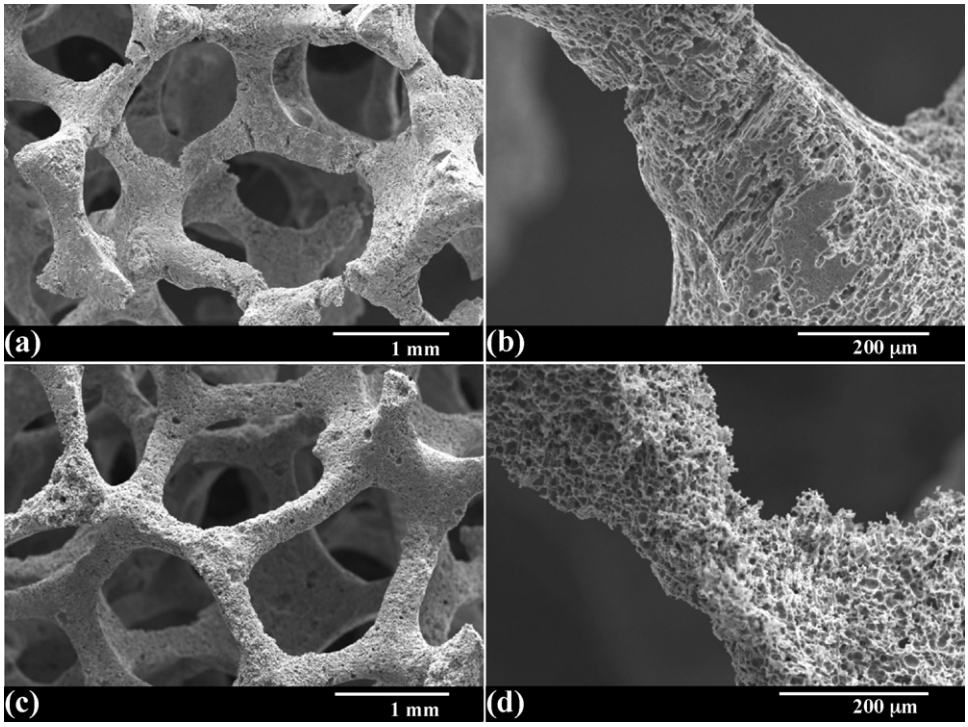

Fig. 4. SEM micrographs of T6- and solution-treated foams with initial relative density of 9.7% after immersion in a pH 2 HCl solution at 23 °C. (a and c) Strut and node surfaces for foams with 7.5% (T6-treated foam) and 8% (solution-treated foam) relative densities, respectively. (b and d) Individual strut of foams with 7.5% (T6-treated foam) and 8% (solution-treated foam) relative densities, respectively.

dictions from SEM examination, though it is noteworthy that the method of calculation of strut thickness is volume-weighted and thus tends to emphasize thicker node-like features, leading to overestimates for strut thickness [13].

More significantly, the difference in mean strut thickness (Table 2) between as-received and moderately dissolved (7.5%) foams is smaller than the difference between moderately to severely dissolved (5%) foams. Due to their higher specific sur-

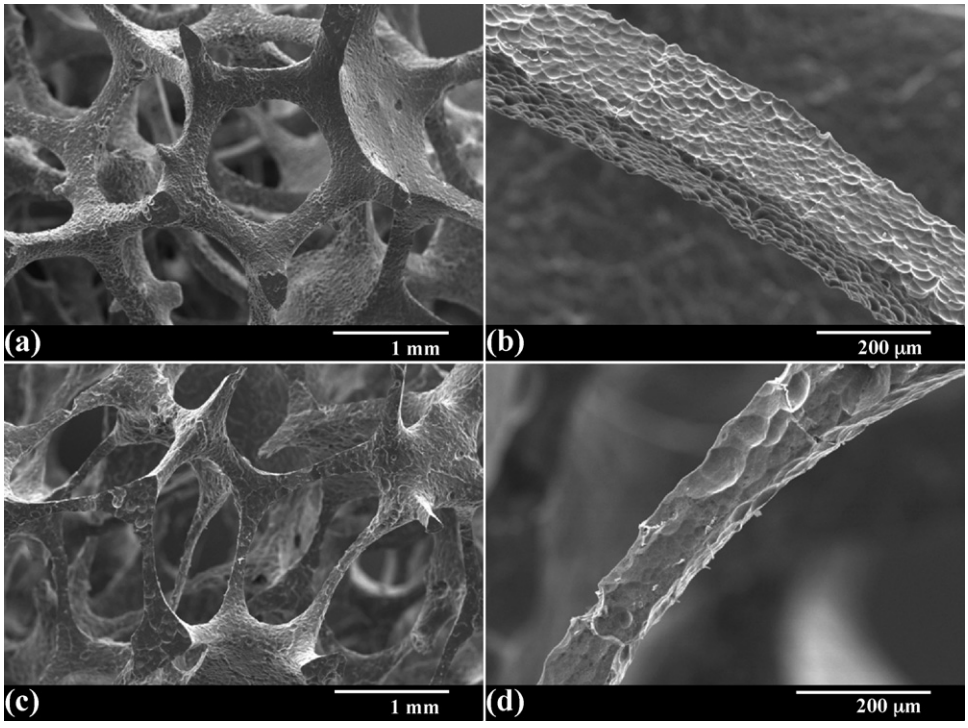

Fig. 5. SEM micrographs of T6-treated foams with initial relative density of 9.5% after immersion in a pH 13 NaOH solution at 23 °C. (a and c) Strut and node surfaces for foams with 7.5 and 5% relative densities, respectively. (b and d) Individual strut of foams with 7.5 and 5% relative densities, respectively.

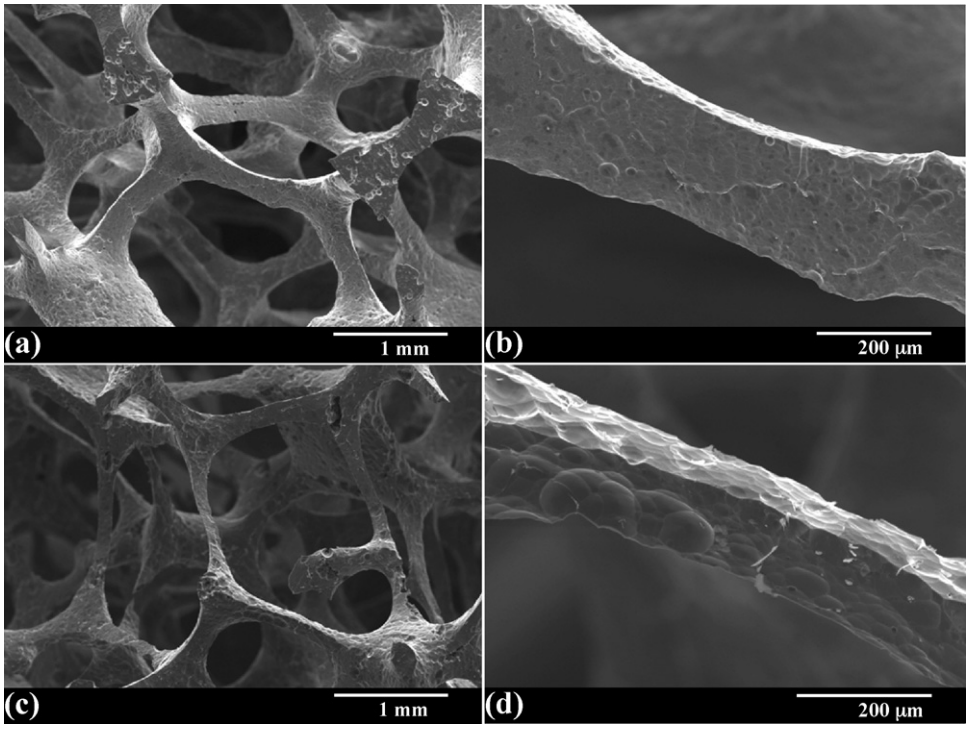

Fig. 6. SEM micrographs of solution-treated foams with initial relative density of 9.7% after immersion in pH 13 NaOH solution at 23 °C. Panels (a and c) illustrate overall structure and surface states in each foam (relative densities: 7.5 and 5%, respectively). Panels (b and d) highlight individual struts in each foam, respectively.

face area (i.e., high aspect ratio), struts may be expected to bear a disproportionate fraction of the total alloy loss, as was apparent in SEM examinations (Figs. 4–6). Consequently, it is also anticipated that relative decreases in strut thickness (reflecting only the dissolution of struts) will outpace those of average foam density (reflecting both struts and more slowly dissolving nodes), as reported previously in amorphous metal foams dissolved in acid solutions [16]. In that study, foam strength also decreased more rapidly with density than in conventional metallic foams, a reflection of the relative importance of struts (as compared to nodes, which deform only slightly at low macroscopic strains) in determining foam mechanical properties.

To quantify the effect of such preferential strut attack more precisely, the non-dimensional structure model index (SMI) of each sample was also calculated, and the results are included in Table 2. The SMI is used to characterize the conformity of the real structure to various model structures, e.g., plates (SMI = 0), cylindrical rods (SMI = 3) or spheres (SMI = 4), based on changes in surface area attending small 'dilations' of the structure outwards along its surface normals [14]. An SMI of 3.25 for the as-received foam is consistent with a structure composed mostly of rods (i.e., struts), with some spherical features (i.e., nodes). Increases in SMI with dissolution indicate evolution towards more spherical features, or a decrease in the proportion of rod-like struts, in agreement with the discussion presented above. The fact that changes in SMI accelerate between 7.5 and 5% relative density again suggests that high levels of dissolution cause proportionally greater changes to foam architecture than moderate degrees of dissolution.

Table 2
Tomographic parameters calculated from three foam specimens, solutionized and then dissolved in room temperature NaOH solution of pH 13

ρ/ρ_s from physical measurement (%)	ρ/ρ_s from μCT (%)	Mean strut diameter (μm)	SMI
9.7	8.9 ± 0.6	289 ± 5	3.25 ± 0.08
7.5	7.9 ± 0.7	273 ± 7	3.29 ± 0.04
5.1	5.1 ± 0.3	233 ± 7	3.58 ± 0.09

Error values represent standard deviations based on five measurements taken along the gauge length of each sample.

3.3. Mechanical properties

In accordance with the observations above, a series of foams with relative densities near 10% (as-received), 7.5, 6.25 and 5% were created by dissolution under minimally damaging conditions (NaOH solutions of pH 13). To further study optimized conditions, specimens were produced using solutions at room temperature and 70 °C, and in both ST and T6 conditions. To investigate the effect of the HCl-induced microstructural damage seen in Fig. 4, ST and T6-treated specimens were also created using room temperature HCl solutions of pH 1. All specimens which had been solutionized prior to dissolution were given a T6 heat-treatment before mechanical testing, in order to standardize the mechanical properties of the strut material.

Compressive yield strength for these foams is compiled as a function of relative density in Fig. 7a. As shown in the figure, there was a noticeable loss of strength in the HCl-treated samples when compared to the NaOH-treated samples. However, among the NaOH-treated samples, there was no significant difference

in strength between samples dissolved in room temperature and 70 °C heated solutions. There was also no consistent difference in strength between foams dissolved in the ST and T6 conditions, despite the differences in strut surface appearance (Figs. 5 and 6). Though more data would be needed to identify subtler differences, these data suggest that the presence of visible cracks, grain pullout, thick corrosion product layers and other forms of severe damage incurred during HCl treatments are sufficient to affect foam strength, as might be expected. By contrast, moderate surface pitting such as that seen in the NaOH-treated specimens did not lead to major changes in foam strength, perhaps due to the relative notch-insensitivity of ductile aluminum struts.

A notable feature of the data, however, is that the relative loss in strength with decreasing density was more rapid than predicted by conventional scaling laws. To illustrate this point, a best-fit line having a slope of 1.5 (corresponding to the exponent of Ashby et al.'s scaling power-law for the strength of open-cell foams of varying density [1]) is provided in Fig. 7a. The data for foams with densities in the range ca. 7–10% could reasonably be fit to such a line, but when data for foams near 5% density are included, a higher slope (the best-fit value found by allowing a variable exponent in the power-law equation) near 4 is suggested. This indicates that modest changes in density (from 10 to 7%) are accommodated without severe damage or fundamental changes to the structure of the foam, whereas more substantial dissolution (to 5–6%) causes strut damage and/or a qualitative change in the shape of the struts themselves. This observation is in agreement with the SEM and tomographic analyses presented in the previous section, as well as with similar accelerated strength losses in amorphous metal foams dissolved in acid baths [16].

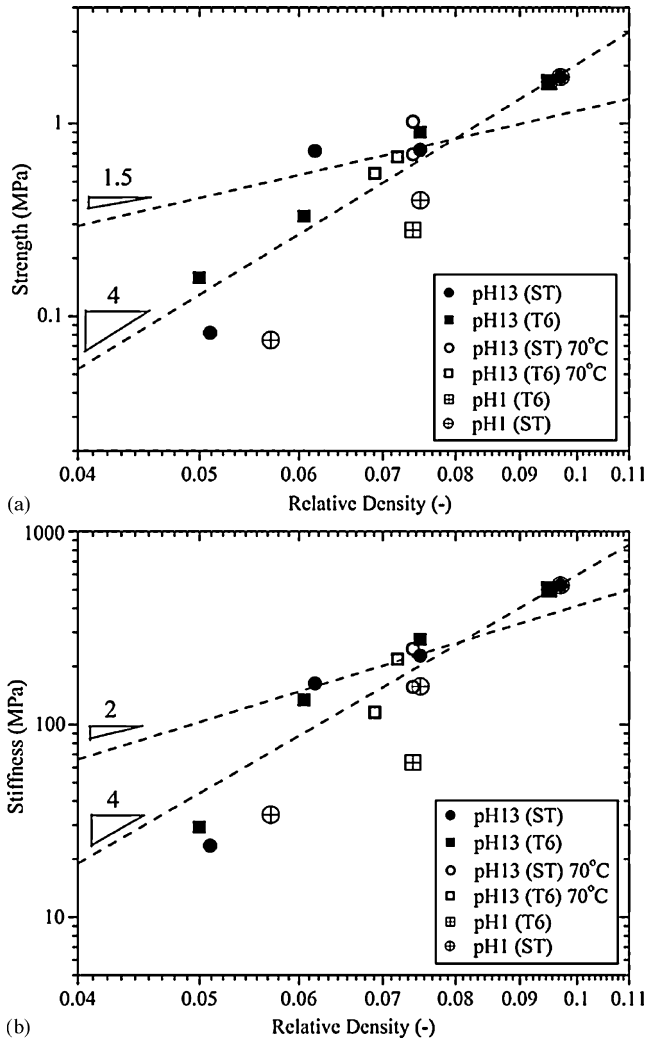

Fig. 7. Effect of relative density on: (a) compressive strength and (b) initial stiffness for foams produced by dissolution in NaOH and HCl solutions. Also shown are best fits using the respective power-law scaling relationships of Ashby et al. [1]. Data were fitted using the commonly accepted exponents for open-cell foams (slopes of 1.5 and 2, respectively), as well as unconstrained best-fit exponents (slopes of 4 in each case). All tested specimens were included during fitting.

Fig. 7b shows initial stiffness for the same series of foams, as a function of relative density. The same trends are apparent, with visible differences between HCl- and NaOH-treated foams, but no significant differences between room temperature and heated NaOH solutions, or between foams dissolved in NaOH in the ST and T6 conditions. Similarly, while the higher-density points (6–7% and higher) could be described by the conventional Gibson–Ashby equation (illustrated by a best-fit line of slope 2), the points near 5% density appear to fall below the prediction, leading again to a higher overall slope of 4 (i.e., a faster loss in stiffness than would be expected from normal foam processing methods). In this case, the deviation from conventional behavior is more pronounced, and occurs quite distinctly between 6.25 and 5%. Thus the foam stiffness data corroborate the observation, suggested by the strength data, that the severity of surface pitting is less important a predictor of mechanical properties for these foams than relative density.

3.4. Density grading

Density grading by dissolution was conducted in pH 13 NaOH solutions at 23 °C, using the process detailed in Section 2.4. The relationship between strut area fraction with standard deviation and the distance from the upper foam edge (unexposed to the solution), estimated by image analysis, is shown in Fig. 8. The cross-section used to determine the strut fraction data is shown in the inset; the vertical left side of this image is the upper part of the sample, and the right side is the lower part, experiencing the shortest and longest immersion, respectively. The measured area fraction changed from 10 to 5% with distance from the upper edge. This decrease appears to be nearly linear, but measurement errors do not allow a precise characterization of the profile. The rapid density change at a 30 mm distance from the sample top was due to strut fracture by excessive dissolution, as well as handling damage, consistent with the study of mechanical properties presented above.

A similar experiment was conducted at 70 °C with a faster rate of change in bath level of 60 mm/h. Although much more rapid density grading was possible in this manner, corrosion damage in the form of pits was more severe, and is expected to lead to reduced mechanical properties. Based on these demonstra-

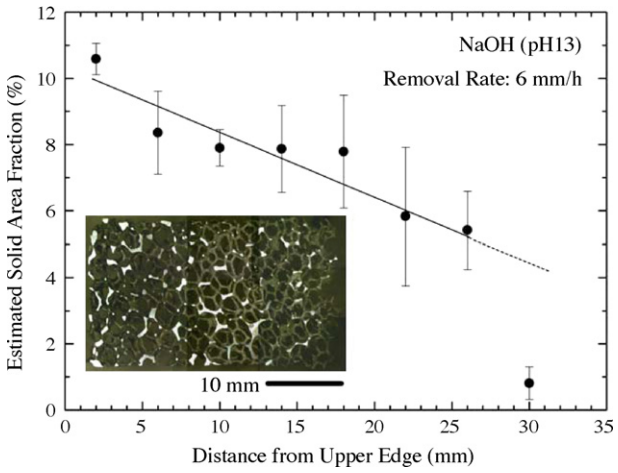

Fig. 8. Relationship between strut area fraction and distance from the upper foam edge for a density-graded foam produced in pH 13 NaOH solution at 23 °C. (Inset) cross-sectional image of sample used for measurements.

tion experiments, it is concluded that optimal control of solution pH and temperature are required in order to reduce foam density while leaving the struts and nodes of density-graded foams intact. However, under such conditions it is believed that density-graded foams with minimum relative densities near 5% can be reliably obtained using this method.

4. Conclusion

Commercial reticulated Al-6101 foams were studied under free dissolution conditions in a series of acidic and alkaline environments. Optimal dissolution conditions, based on visual and quantitative evaluation of damage combined with mechanical property evaluation, were identified in solution-treated foams dissolved in room temperature NaOH solutions of pH 13. Mechanical properties were also evaluated under several other dissolution conditions, and foam strength and stiffness were generally found to decrease more rapidly with density than is typical for metallic foams, especially in highly damaging acidic baths and for heavily dissolved samples, where preferential strut thinning led to microstructural damage. Nevertheless, under optimal conditions, continuous density gradients from approximately 10 to 5% relative density could be successfully produced in originally uniform-density commercial foams.

Acknowledgements

The authors thank Dr. O. Couteau (formerly of Northwestern University) for helpful discussions, and Mr. Joe Doll of ERG Aerospace for generously providing the Duocel® aluminum foams used in this study. The authors also gratefully acknowledge financial support from the U.S. Department of Energy via the University of California, Lawrence Livermore National Laboratories, under contract W-7405-Eng-48 and administered by Dr. A.M. Hodge.

References

[1] M.F. Ashby, A.G. Evans, N.A. Fleck, L.J. Gibson, J.W. Hutchinson, H.N.G. Wadley, Metal Foams: A Design Guide, Butterworth-Heinemann, Boston, 2000.
[2] G.J. Davies, Shu Zhen, J. Mater. Sci. 18 (1983) 1899–1911.
[3] T. Daxner, F.G. Rammerstorfer, H.J. Böhm, Mater. Sci. Technol. 16 (2000) 935–939.
[4] A. Pollien, Y. Conde, L. Pambaguian, A. Mortensen, Mater. Sci. Eng. A 404 (2005) 9–18.
[5] Y. Conde, A. Pollien, A. Mortensen, Scripta Mater. 54 (2006) 539–543.
[6] H. Togashi, K. Yuki, H. Hashizume, Fusion Sci. Technol. 47 (2005) 740–745.
[7] C. Solaiyan, P. Gopalakrishnan, S. Dheenadayalan, I. Arul Raj, S. Muzhumathi, R. Chandrasekaran, R. Pattabiraman, Indian J. Chem. Technol. 6 (1999) 48–54.
[8] H.C. Shin, J. Dong, M.L. Liu, Adv. Mater. 15 (2003) 1610–1614.
[9] A. Neubrand, J. Appl. Electrochem. 28 (1998) 1179–1188.
[10] F.-W. Bach, D. Bormann, P. Wilk, in: J. Banhart, N.A. Fleck, A. Mortensen (Eds.), Proceedings of the Third International Conference on Cellular Metals and Metal Foaming Technology (MetFoam 2003), MIT-Verlag, Berlin, Germany, 2003, pp. 215–218.
[11] A.H. Brothers, D.C. Dunand, Adv. Eng. Mater. 8 (2006) 805–809.
[12] J. Bray (Ed.), Aluminum Mill and Engineered Wrought Products, ninth ed., ASM International, Materials Park, OH, 1990.
[13] T. Hildebrand, P. Rüegsegger, J. Microsc. 185 (1997) 67–75.
[14] T. Hildebrand, P. Rüegsegger, Comp. Meth. Biomech. Biomed. Eng. 1 (1997) 15–23.
[15] S. Sakashita, T. Nakayama, N. Ibaraki, K. Ochiai, Kobe Steel Eng. Rep. 50 (2000) 61–64 (in Japanese).
[16] A.H. Brothers, D.C. Dunand, Acta Mater. 53 (2005) 4427–4440.